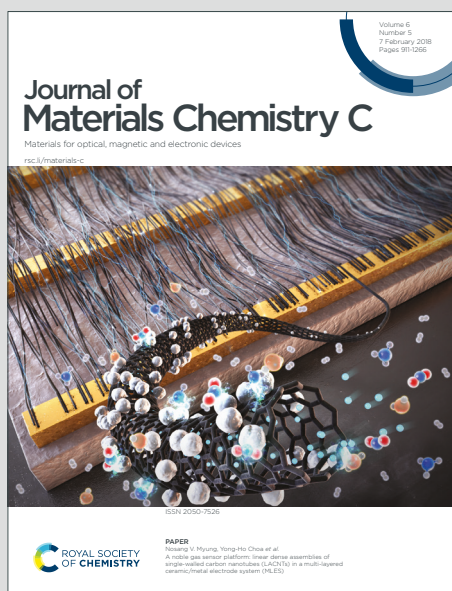


Journal of Materials Chemistry C

Materials for optical, magnetic and electronic devices

Accepted Manuscript

This article can be cited before page numbers have been issued, to do this please use: J. Yang, X. Liu, Z. Liu, L. Wang, J. Sun, Z. Guo, H. Xu, H. Wang, B. Zhao and G. Xie, *J. Mater. Chem. C*, 2020, DOI: 10.1039/C9TC06425G.



This is an Accepted Manuscript, which has been through the Royal Society of Chemistry peer review process and has been accepted for publication.

Accepted Manuscripts are published online shortly after acceptance, before technical editing, formatting and proof reading. Using this free service, authors can make their results available to the community, in citable form, before we publish the edited article. We will replace this Accepted Manuscript with the edited and formatted Advance Article as soon as it is available.

You can find more information about Accepted Manuscripts in the [Information for Authors](#).

Please note that technical editing may introduce minor changes to the text and/or graphics, which may alter content. The journal's standard [Terms & Conditions](#) and the [Ethical guidelines](#) still apply. In no event shall the Royal Society of Chemistry be held responsible for any errors or omissions in this Accepted Manuscript or any consequences arising from the use of any information it contains.

ARTICLE

Protonation-Induced Dual Fluorescence of a Blue Fluorescence Material with Twisted A- π -D- π -A ConfigurationReceived 00th January 20xx,
Accepted 00th January 20xxJingjing Yang^a, Xing Liu^a, Zemei Liu^a, Long Wang^a, Jing Sun^a, Zhen Guo^b, Huixia Xu^a, Hua Wang^{*ac}, Bo Zhao^{*a}, Guohua Xie^{*d}

DOI: 10.1039/x0xx00000x

In this work, we introduced a blue fluorescence material with twisted A- π -D- π -A configuration, namely **CzPA-F-PD**. This compound exhibits remarkable dual fluorescence properties triggered by trifluoroacetic acid (TFA), resulting in blue and red emission peaks under both the photoluminescent and electroluminescent processes. The reversibility of dual fluorescence can be triggered by neutralizing TFA with triethylamine (TEA). By spectral measurement and analysis, it is identified that hydrogen protonation of TFA amplifies the lone pair electrons around nitrogen atoms in pyridine and enhances electron acceptor ability, which play a major role during dual fluorescence process. In addition, **CzPA-F-PD** can be used as a sensitive fluorescent probe for pH monitoring. Furthermore, **CzPA-F-PD** can also serve as the white emission single layer with some amount of TFA in solution-processed OLED, which expresses CIE coordinates of (0.36, 0.37) and a high current efficiency of 6.37 cd/A. Unprecedentedly, the high single exciton utilization efficiency is up to 67.8%, exceeding the upper limit (25%) of the traditional fluorescence material.

Introduction

Organic dual fluorescence materials (ODFMs) possess the unique properties such as double emission peaks that cover visible emission spectrum, high spectral sensitivity to the surrounding environment, ease of fabrication over multicomponent systems and rapid response.¹⁻³ Hence, ODFMs have acquired enormous interest in white organic light-emitting device (WOLED),⁴⁻⁶ fluorescent probe,⁷ cell bio-imaging,⁸ molecular logic gate,^{9, 10} anti-counterfeiting coding, etc.¹¹

Generally, the molecule showing dual fluorescence usually involves a mixture of the excited states or conformational equilibrium in the excited state or ground state.¹²⁻¹⁴ Recently, many efforts have been made to develop effective methods for acquiring ODFMs, for example, partial intermolecular Förster resonance energy transfer,¹⁵⁻¹⁷ excited state intramolecular proton transfer (ESIPT),¹⁸⁻²⁰ and twisted intramolecular charge transfer (TICT).^{6, 21} Up to date, many ODFMs have been reported to realize dual fluorescence emission through above methods successfully. For practical application, there exist many problems to be solved. Firstly, owing to the unfavorable excited state energy exhausted in non-

radiative process for obtaining dual fluorescence emission, ODFMs usually exhibit relatively lower luminescence efficiency. Secondly, ODFMs realize dual fluorescence emission through two radiative transition paths of two isomeric excited state molecules, which means that it is rather challenging to adjust dual fluorescence intensity owing to difficulty in controlling the ratio of two isomeric excited state molecules.^{1, 22}

In our previous work, we designed and synthesized the blue fluorescence material of **CzPA-F-TFMP** with twisted A- π -D- π -A structure, in which N-(4-aminophenyl)carbazole (CzPA) served as electron donor (D) unit, trifluoromethylphenyl (TFMP) as electron acceptor (A) unit, and 9,9-dioctylfluorene (F) as π -conjugated unit, respectively.²³ **CzPA-F-TFMP** exhibits higher external quantum efficiency (EQE) that exceeds the theoretical upper limit (5%) of the classical fluorescence material, owing to partial separation between the highest occupied molecular orbital (HOMO) and the lowest unoccupied molecular orbital (LUMO).²⁴⁻²⁶ Hence, to improve the luminescence efficiency of ODFMs, we designed and developed the ODFMs, i.e., **CzPA-F-PD**, with twisted A- π -D- π -A structure in this work. Distinguished with **CzPA-F-TFMP**, the pyridine (PD) served as electron acceptor unit. PD unit is a nitrogen-based π -deficient heterocycle, which can enhance electron acceptor ability by engaging lone pair electrons around nitrogen atoms through hydrogen protonation.²⁷⁻³¹ It can lead to red-shift of photoluminescence spectra of **CzPA-F-PD** in acid surrounding and realize dual fluorescence emission. Based on it, solution-processed WOLED have been realized by doping a certain amount of acid into thin films of pyridine derivatives and a fluorescence probe for pH sensing was constructed. Above preliminary results revealed that the **CzPA-F-PD** has potential applications in optoelectronic devices and sensors.

^a Key Laboratory of Interface Science and Engineering in Advanced Materials, Ministry of Education, Taiyuan University of Technology, Taiyuan 030024, P.R. China. *E-mails: wanghua@tyut.edu.cn; zhaobo01@tyut.edu.cn

^b College of Material Science & Engineering, Taiyuan University of Technology, Taiyuan, Taiyuan 030024, P.R. China.

^c College of Textile Engineering, Taiyuan University of Technology, Taiyuan, Taiyuan 030024, P.R. China.

^d Sauvague Center for Molecular Sciences, Hubei Key Lab on Organic and Polymeric Optoelectronic Materials, Department of Chemistry, Wuhan University, Wuhan 430072, P.R. China.

*E-mail: guohua.xie@whu.edu.cn

†Electronic Supplementary Information (ESI) available.

Experimental section

Synthetic section

All organic chemicals and solvents were received from commercial sources and used, unless otherwise noted, without further purification. The synthetic route of **CzPA-F-PD** is shown in Scheme 1. The intermediate products of 9-(4-nitrophenyl)-9H-carbazole (**1**) and 4-(9H-carbazol-9-yl) aniline (**2**) were synthesized according to reference.²³

CzPA-F-Br. The **CzPA-F-Br** was synthesized by Ullmann reaction. The compound of **2** (0.54 g, 2.11 mmol), 2,7-dibromo-9,9-dibutyl-9H-fluorene (2.76 g, 6.33 mmol), sodium tert-butoxide (NatB) (1.02 g, 10.55 mmol), 1,1'-bis(diphenylphosphino)ferrocene (DPPF) (0.061 g, 0.11 mmol) and Pd₂(dba)₃ (0.10 g, 0.11 mmol) were added into toluene (20 mL) and mixed uniformly. Under nitrogen protection, the mixture was stirred and refluxed at 110 °C for 24 h. After cooling to room temperature, the reaction mixture was washed by water and extracted with dichloromethane consecutively. The organic phase was collected and further dried with anhydrous MgSO₄. After rotary evaporation of solvent, the residue was purified via column chromatography by using n-hexane as eluent to give intermediate products of **CzPA-F-Br** (0.92 g, yield: 45%). ¹H NMR (600 MHz, CDCl₃, δ): 8.15 (d, J = 7.8 Hz, 2H), 7.60 (d, J = 8.1 Hz, 2H), 7.54 – 7.37 (m, 12H), 7.31 (dt, J = 14.8, 7.5 Hz, 4H), 7.24 (s, 2H), 7.20 – 7.09 (m, 2H), 1.90 (m, J = 7.2, 3.0 Hz, 8H), 1.16 – 1.07 (m, 8H), 0.78 – 0.64 (m, 20H).

CzPA-F-PD. The **CzPA-F-Br** (0.97 g, 1 mmol), 4-pyridineboronic acid pinacol ester (0.82 g, 4 mmol) and Pd(PPh₃)₄ (0.06 g, 0.05 mmol) were added to a mixed solution of toluene (20 ml) and aqueous solution of K₂CO₃ (5 mL, 2 M). The mixture was heated at 110 °C and refluxed under nitrogen protection for 12 h. Then, the reaction was quenched by water and extracted with dichloromethane. The organic phase was collected and dried over anhydrous MgSO₄. After removing solvent by rotary evaporation, the residue was purified via column chromatography. The petroleum ether / ethyl acetate (2:1, v/v) were used as eluent to afford yellow solid of **CzPA-F-PD** (0.61 g, yield: 63%). ¹H NMR (600 MHz, CDCl₃, δ): 8.68 (m, 4H), 8.16 (d, J = 7.7 Hz, 2H), 7.75 (d, J = 7.9 Hz, 2H), 7.69 (d, J = 8.2 Hz, 2H), 7.65 (dd, J = 7.9, 1.7 Hz, 2H), 7.61 – 7.58 (m, 6H), 7.49 (d, J = 8.2 Hz, 2H), 7.46 – 7.42 (m, 4H), 7.39 – 7.36 (m, 2H), 7.33 – 7.29 (m, 4H), 7.21 (dd, J = 8.2, 2.1 Hz, 2H), 2.05 – 1.94 (m, 8H), 1.17 – 1.08 (m, 8H), 0.74 (t, J = 7.4 Hz, 20H). ¹³C NMR (151 MHz, CDCl₃, δ): 155.75, 154.58, 153.19, 151.58, 150.20, 144.89, 143.95, 139.17, 138.87, 134.60, 130.68, 129.03, 128.78, 126.88, 126.70, 126.26, 124.44, 124.08, 123.92, 123.27, 122.78, 122.71, 122.29, 112.68, 58.21, 42.91, 29.10, 25.93, 16.82. Elem. anal. Found: C, 87.88; H, 7.301; N, 7.43. Calcd for **CzPA-F-PD**: C, 87.10; H, 7.10; N, 5.80. HRMS (MALDI) calcd. for **CzPA-F-PD**: 964.540; found: 964.250.

Molecule and properties

The molecular structure of **CzPA-F-PD** was confirmed by ¹H NMR, ¹³C NMR and mass spectra. The ¹H and ¹³C NMR data were acquired on Bruker DRX 600 spectrometer at 600 MHz and 151 MHz respectively. Mass spectrometry was recorded on ultrafleXtreme MALDI TOF/TOF. Furthermore, elemental analysis was acquired on vario EL cube, ELEMENTAR.

The ultraviolet visible (UV-vis) absorption spectra were measured using a Hitachi UV-vis spectrometer 3900. The photoluminescence (PL) spectra were acquired on Horiba Fluoromax-4 spectrophotometer. The fluorescence lifetime and absolute fluorescence quantum yield were obtained by Edinburgh FLS980 steady state fluorimeter equipped with integrating sphere. Thermogravimetric analysis (TGA) was performed on a Netzsch TG 209F3 thermal analyzer under a nitrogen atmosphere at a heating rate of 10 °C/min from 30 °C to 790 °C. The energy levels and electrochemical properties were studied by cyclic voltammetry (CV) in dichloromethane (DCM) solution and 0.1M tetrabutylammonium perchlorate as the supporting electrolyte. The single crystal of **CzPA-F-PD** was cultured by vapour diffusion of DCM solution and acetonitrile. Diffraction data were collected on XtaLAB Synergy R, HyPix diffractometer. The single crystal of **CzPA-F-PD** was kept at 220.00(13) K during data collection.

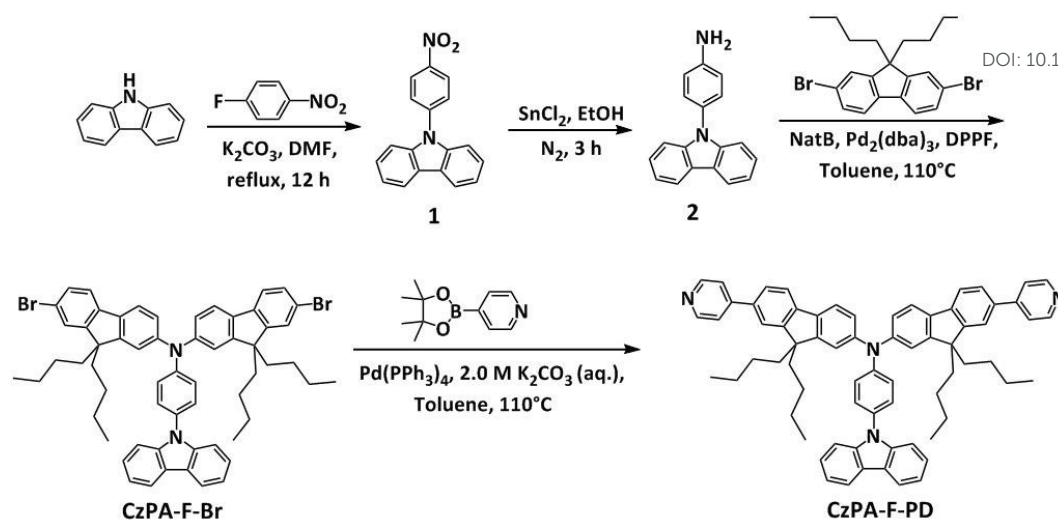
OLED fabrication

The OLED were fabricated on ITO glass substrates with a sheet resistance of 10 Ω/sq, which were cleaned and irradiated by ultraviolet before fabrication. Next, the PEDOT: PSS was spin-coated onto the treated ITO glass substrates in a glove box, annealed at 120 °C for 20 minutes. Then the solutions of **CzPA-F-PD** in chlorobenzene (10 mg/mL) and TFA were prepared according to volume ratios of **CzPA-F-PD**:TFA (50/1, v:v), **CzPA-F-PD**:TFA (5000/1, v:v), and **CzPA-F-PD**, respectively. The solutions were then spin-coated to form the emission layers, followed by the thermal annealing at 50 °C for 10 minutes. After that, bis[2-(diphenylphosphino)phenyl]ether oxide (DPEPO), 1,3,5-tri(mpyridin-3-ylphenyl)-benzene (TmPyPB), 8-quinolinolalolithium (Liq) and aluminium (Al) were sequentially thermal evaporated onto emission layer in a vacuum evaporation equipment at 5×10⁻⁴ Pa. After the fabricating OLED, the luminance and electroluminescence (EL) spectra and chromaticity coordinates were measured using PR-735 scan spectrometer. Simultaneously, the current and voltage were obtained by a Keithley 2400 source. The current and power efficiencies were calculated from the J-V-L characteristic curves. The EQE was calculated by combining the J-V-L characteristic curve and EL spectrum. All measurements were made at room temperature under ambient conditions after encapsulating the devices with the UV epoxy.

Results and discussion

Single crystal structure

Single crystals structure of **CzPA-F-PD** was determined by single-crystal X-ray diffraction analysis. And, detail crystal structure data were list in Table S1 (ESI*). Seeing in Fig. 1a, **CzPA-F-PD** shows rather smaller twisting angle of 20° between PD unit and fluorene ring, which makes large π conjugated skeleton; rather bigger twisting angle of 52° between carbazole unit and phenyl ring, which is due to strong repulsion between two adjacent hydrogen atoms in carbazole and phenyl ring. So, it is indicated twisting A-π-D-π-A conformation of **CzPA-F-PD**. In addition, it can be found in Fig. 1b that **CzPA-F-PD** molecules adopt antiparallel coupling and establish efficient tail-to-tail interaction with adjacent molecules through C-H.....π (2.895 Å)



Scheme 1. Synthetic routes of CzPA-F-PD.

and C–H.....H hydrogen bonds (2.323 Å) in each layer. Such interactions help to solidify the molecular conformation and block non-radioactive pathways, which had led to high fluorescence quantum yield (η_{pl}) of CzPA-F-PD.^{32, 33}

Photophysical properties

The UV-vis absorption and PL spectra of CzPA-F-PD are shown in Fig. 2. The UV-vis absorption spectrum in chloroform (CHCl_3) solution expresses three absorption peaks located at 243, 296 and 384 nm, attributing to $\pi\text{-}\pi^*$ transition of benzene rings, $n\text{-}\pi^*$ transition of CzPA, charge transfer (CT) from electron donor unit of CzPA to electron acceptor unit of PD, respectively.^{23, 34, 35} The PL spectrum of CzPA-F-PD in CHCl_3 solution exhibits emission peak (λ_{pl}) at 470 nm, corresponding to blue-emission originated from CT from CzPA to PD. Furthermore, it can be found that the UV-vis absorption and PL spec-

tra of CzPA-F-PD film is nearly identical with those of CzPA-F-PD in CHCl_3 solution. The reason might be weaker intermolecular $\pi\text{-}\pi$ interaction induced by the bigger steric hindrance of CzPA-F-PD molecule and longer butyl chains. Hence, the CzPA-F-PD in solution exhibits rather higher η_{pl} of 67%, CzPA-F-PD film also shows rather higher η_{pl} of 52.9%.

Subsequently, the excited state character of CzPA-F-PD was studied following the method introduced in our early work.^{23, 36} As presented in Fig. S7 and S8 (ESI*), it can be suggested that the excited state of CzPA-F-PD possess a major charge transfer (CT) state character combining with the local excited (LE) state character.^{23, 24} Meanwhile, the electronic density distribution of the frontier molecular orbitals was fully constructed by the density functional theory (DFT) calculations with B3LYP hybrid functional at the basis set level of 6-31G (d, p) under Gaussian 09 package. In Fig. 9, it can be seen that the HOMO is mainly delocalized on CzPA unit; LUMO is nearly covered whole π -conjugated skeleton composed of two pyridine units and two fluorene units; there exists obvious separation between HOMO and LUMO, owing to its twisting molecular structure identified by single crystal structure; there also exists obvious overlap between HOMO and LUMO localized on two fluorene units. Meanwhile, this is more likely to endow the excited states of CzPA-

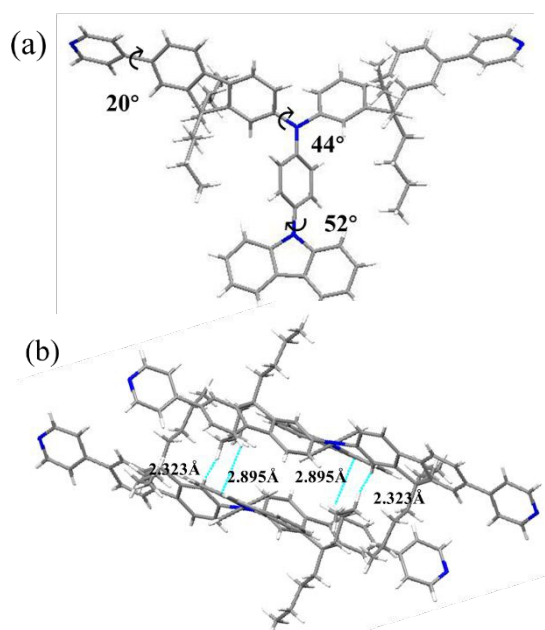


Fig. 1 (a) Single crystal structure of CzPA-F-PD. (b) Intermolecular interactions in the crystal packing diagram of CzPA-F-PD.

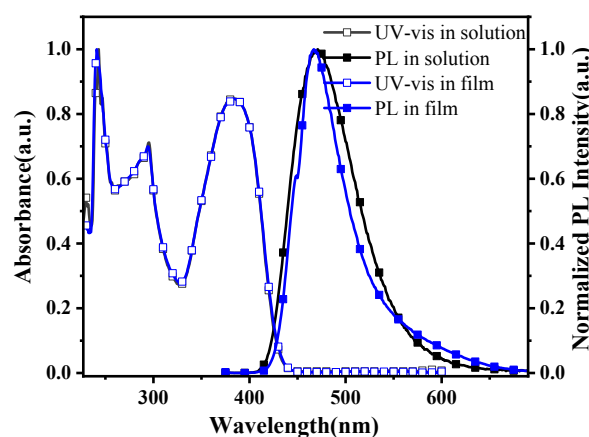


Fig. 2 The UV-vis absorption and PL spectra of CzPA-F-PD in CHCl_3 solution with concentration of 10^{-5} mol/L and CzPA-F-PD film.

F-PD with both CT and LE characters. Therefore, it is deduced that **CzPA-F-PD** possesses higher single exciton utilization efficiency (η_s) above upper limit of 25% and higher η_{PL} , which means higher EQE when it is used in OLED.

Dual fluorescence properties

In **CzPA-F-PD** molecule, the PD unit is a nitrogen-based π -deficient heterocycle. The lone pair electrons surrounding nitrogen atoms of PD unit can be enlarged by binding with hydrogen protons, to form PD-H⁺ unit.^{16, 17, 37, 38} It will improve electron acceptor ability of PD unit and induce in bathochromic-shift of emission spectrum eventually. Hence, it is suggested that **CzPA-F-PD** can realize dual fluorescence emission by adjusting hydrogen protonation of PD unit facilely. In many reports,^{28, 29} the TFA is usually utilized for hydrogen protonation of pyridine derivatives. Thus, in this work, we mainly induce **CzPA-F-PD** to emit dual fluorescence by introducing TFA.

For testifying the dual fluorescence properties of **CzPA-F-PD**, TFA was gradually added into CHCl₃ solution of **CzPA-F-PD**. The relationship between the photophysical properties and the amount of TFA was studied. In UV-vis absorption spectrum (Fig. 3a), with the increasing amount of TFA, the absorption peak located at 384 nm corresponding to CT from CzPA to PD is weakened. However, the new absorption peak located at 445 nm corresponding to CT from CzPA to PD-H⁺ emerges. In PL spectrum (Fig. 3b), with the increasing amount of TFA, the intensity of blue-emission peak located at 470 nm degrades. Meanwhile, the red-emission peak located at 645 nm appears and intensifies. Therefore, it is identified that **CzPA-F-PD** exhibits remarkable dual fluorescence properties, which can be adjusted by controlling the amount of TFA. As shown in inset of Fig. 3b, under irradiation of UV light, the fluorescence colour of **CzPA-F-PD** in CHCl₃ solution varies from blue, to white, to red, with increasing the amount of TFA. The **CzPA-F-PD** can also be responsive to other acids such as acetic acid (HOAc) and hydrochloric acid (HCl), which exhibit significant dual fluorescence as shown in Fig. S10 (ESI*).

Furthermore, the dual fluorescence properties of **CzPA-F-PD** film were investigated. As presented in Fig. 4b, the **CzPA-F-PD** film also shows spectral response characteristics to TFA. The λ_{PL} in PL spectrum of **CzPA-F-PD** film red-shifts from 468 nm to 635 nm after fuming with TFA vapor for ten seconds. And, fluorescence emission colour of **CzPA-F-PD** film changes from blue to red by fuming with

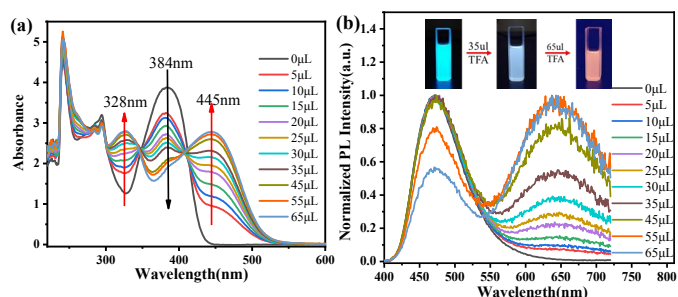


Fig. 3 Photophysical properties of **CzPA-F-PD** in CHCl₃ solution (3 mL, 10⁻⁵ mol/L) with different amount of TFA (0.0013 mol/L): (a) UV-vis absorption spectrum; (b) PL spectrum, inset is photographs of **CzPA-F-PD** in CHCl₃ solution containing different amounts of TFA under irradiation of UV light.

TFA vapor as showing in inset of Fig. 4b.

Following, basic solvent of TEA was dropped into the CHCl₃ solution of **CzPA-F-PD** containing TFA (10.0 equiv.), which can realize deprotonation of **CzPA-F-PD-H⁺**. In Fig. 5a and 5b, it can be found that the UV-vis absorption and PL spectra of **CzPA-F-PD-H⁺** in CHCl₃ solution nearly reverse to original shape of **CzPA-F-PD** after dropping TEA. Hence, it is suggested that **CzPA-F-PD** in CHCl₃ solution exhibits dual fluorescence reversibility by dropping TFA and TEA alternately. More specially, **CzPA-F-PD** film shows remarkable reversibility of dual fluorescence. As shown in Fig. 5c, upon fuming with TFA and TEA vapor alternately, the λ_{PL} in PL spectrum of **CzPA-F-PD** film varies between 470 nm and 650 nm in turn, inducing in alternation of fluorescence colour between blue and red. In addition, the dual fluorescence reversibility phenomena can repeat more than nine cycles. Based on perfect dual fluorescence properties, it can be speculated that **CzPA-F-PD** express huge utilization potential in anti-counterfeiting technology.

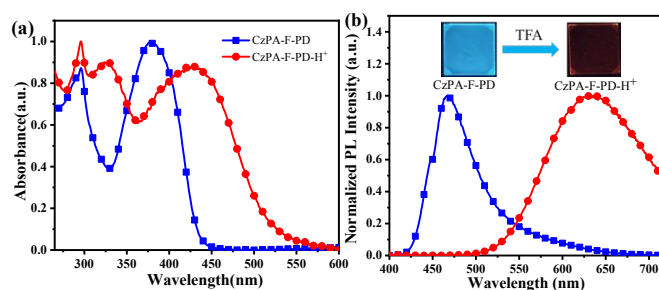


Fig. 4 The UV-vis absorption (a) and PL spectra (b) of **CzPA-F-PD** film and **CzPA-F-PD-H⁺** film. Inset is photographs of **CzPA-F-PD** and **CzPA-F-PD-H⁺** films.

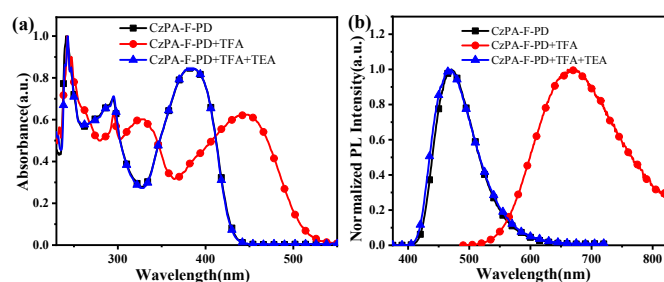


Fig. 5 The UV-vis absorption (a) and PL spectra (b) of **CzPA-F-PD** in CHCl₃ solution upon continuous addition of TFA, TEA. (c) The emission wavelength change of **CzPA-F-PD** films on repeated exposure to TFA and TEA, respectively.

Luminescence mechanism of dual fluorescence

Based on above discussion results, it is testified that **CzPA-F-PD** exhibits remarkable dual fluorescence properties. Following, the luminescence mechanism of dual fluorescence will be analysed in detail.

First of all, **CzPA-F-PD** molecule possesses large π -conjugated skeleton as identified by single crystal diffraction analysis. Thus, it is assumed that the red-light in dual fluorescence of **CzPA-F-PD** might be owing to excimers of adjacent **CzPA-F-PD** molecules.³⁹ For eliminating it, the PL spectra of **CzPA-F-PD** in CHCl_3 solution with increasing concentrations were recorded as shown in Fig. 6.⁴⁰ It can be seen that all PL spectra exhibit one blue-emission peak at 470 nm even under high concentration of 10^{-3} mol/L and none red-emission peak. Additionally, as expressed in crystal packing diagram of **CzPA-F-PD** in Fig. 1b, it is found that the **CzPA-F-PD** molecule is difficulty in forming good molecule packing owing to separation of long alky chains, which restrain formation of excimer.

Secondly, according to the reference work,⁴¹ the 9,9-bioctylfluorene is easily oxidized to form fluorenone, generating long wavelength emission peaks located at around 550 nm in PL spectrum. Because of two 9,9-bioctylfluorene units in **CzPA-F-PD**, it might be another possible reason of dual fluorescence emission of **CzPA-F-PD**. For ruling out it, the PL spectrum of **CzPA-F-PD** film in oxygen atmosphere was acquired and shown in Fig. 7. After being exposed in oxygen atmosphere for 20 minutes, we found that the PL spectrum of **CzPA-F-PD** film under oxygen atmosphere shows only one emission peak at 470 nm that is similar to that of original **CzPA-F-PD** film. It is since that 9,9-bioctylfluorene in **CzPA-F-PD** can't be oxidized owing to strong electron acceptor ability of PD unit, especially being protonated with hydrogen protons. Therefore, it is testified that the 9,9-bioctylfluorene does no contribution to dual fluorescence emission of **CzPA-F-PD**.

For identifying hydrogen protonation on PD unit, we prepared **CzPA-F-PD-H⁺** by dropping excess amount of TFA into CHCl_3 solution of **CzPA-F-PD**.³⁸ By comparing with ^1H NMR spectra of **CzPA-F-PD-H⁺** and **CzPA-F-PD**, it is found that the chemical shifts for the H atoms in pyridine groups significantly downfield shift. For example, as shown in Fig. 8, H₁/H₂ in the ^1H NMR spectra of **CzPA-F-PD** was corresponding to the PD units. The signal of H₁ in PD unit was shifted from 8.68 ppm to 8.88 ppm, and the signal of H₂ was shifted from 7.60 ppm to 8.10 ppm, respectively. It is speculated that the proton

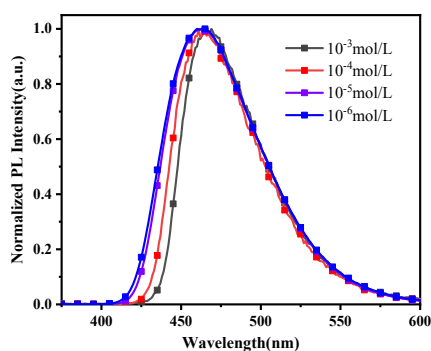


Fig. 6 The PL spectrum of **CzPA-F-PD** in CHCl_3 solution with increasing concentrations.

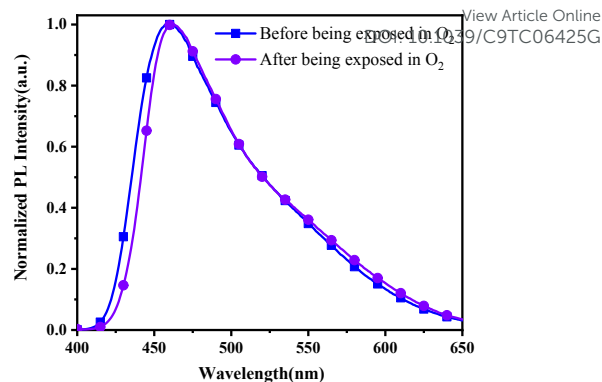


Fig. 7 The PL spectrum of **CzPA-F-PD** films before and after being exposed in O_2 for 20 minutes (Excitation wavelength is 365 nm).

binding of **CzPA-F-PD** is attributed to protonation of the nitrogen atom in the PD unit primarily. Furthermore, the ^1H NMR titration experiments were carried out, which revealed noticeable interaction of **CzPA-F-PD** with TFA. As shown in Fig. S9 (ESI*), the result shows that the dropping of TFA caused obvious downfield shifts of the chemical shifts, particularly at pyridine ring, in line with the change of the acidified molecule and neutral form.

In addition, to investigate the changes in electronic properties of **CzPA-F-PD** upon hydrogen protonation, according reported calculating methods, theoretical calculations were also performed according to DFT at the level of B3LYP/6-31G*.¹⁷ The electronic distribution of HOMO and LUMO of **CzPA-F-PD-H⁺** is shown in Fig. 9. The HOMO is delocalized on CzPA unit and the LUMO is only delocalized on two PD-H⁺ units, which show remarkable separation. It is distinguished with partial overlap between HOMO and LUMO of **CzPA-F-PD**. It had been identified that increasing separation between HOMO and LUMO can lead to strengthen CT-state characteristic and weaken LE-state characteristic of excited state, inducing in red-shift of PL spectrum.^{36,42} Hence, it is suggested that hydrogen protonation on PD unit in **CzPA-F-PD** can improve CT-state emission, which plays major role of red-emission of **CzPA-F-PD-H⁺**. In addition, in our early report,²³⁻²⁵ it had been testified that enhancements of CT-state characteristic also lead to lower η_{PL} of fluorescence material. Thus, hydrogen protonation of **CzPA-F-PD** will also reduce η_{PL} , e.g., the η_{PL} of **CzPA-F-PD** and **CzPA-F-PD-H⁺** are 67.7% and 15.5%.

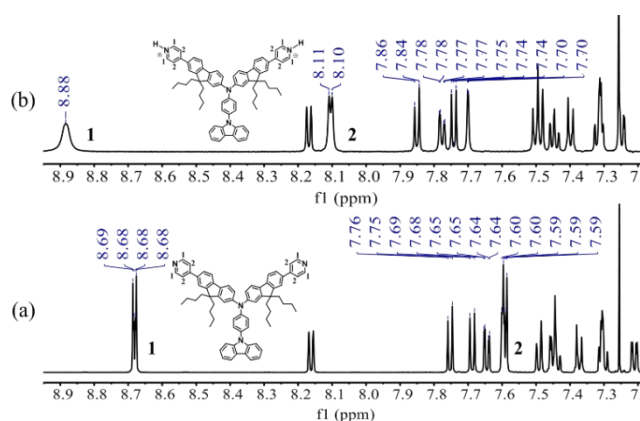
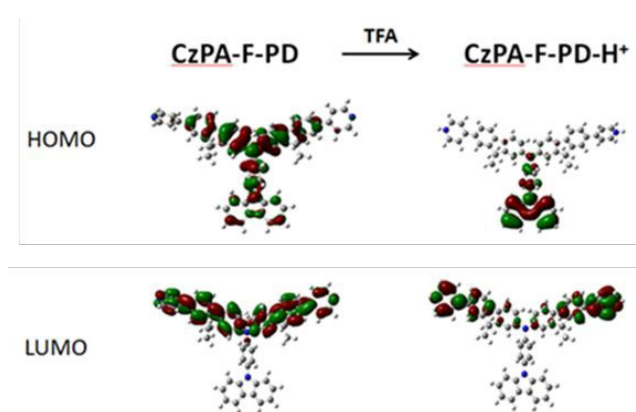


Fig. 8 Partial ^1H NMR chart of (a) **CzPAF-PD** and (b) **CzPAF-PD-H⁺**.

Table 1 The photophysical properties of **CzPA-F-PD** and **CzPA-F-PD-H⁺**

Compound	λ_{abs}^b (nm)	λ_{pl}^b (nm)	λ_{abs}^c (nm)	λ_{pl}^c (nm)	HOMO/LUMO ^d (eV)	E_g^d (eV)	S_1/T_1 (eV)	ΔE_{ST} (eV)	η_{PL}^e (%)	η_{PL}^c (%)	τ_{F}^b (ns)
CzPA-F-PD	243,296,384	470	241,295,383	467	-5.35/-2.46	2.89	2.76/2.37	0.39	67.7	52.9	2.10
CzPA-F-PD-H⁺a	242,295,328,446	620	295,328,430	635	-5.51/-3.24	2.27	2.32/2.16	0.16	15.5	7.90	2.28

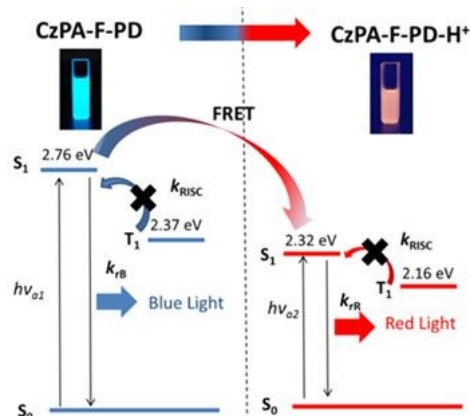
^a **CzPA-F-PD-H⁺** was acquired upon adding 10 equiv of TFA into CHCl_3 solution of **CzPA-F-PD**. ^b Measured in CHCl_3 solution with the concentration of 10^{-5} mol/L (Excitation wavelength is 365 nm). ^c Measured in pure film. ^d Calculated from CV, reference electrode: Fc/Fc^+ (see supporting information for details). ^e Quantum yield (η_{PL}) from the CHCl_3 solution.

**Fig. 9** Spatial distribution of the HOMO and LUMO orbitals of **CzPA-F-PD** and **CzPA-F-PD-H⁺**.

The cyclic voltammograms (CV) curve of **CzPA-F-PD** and **CzPA-F-PD-H⁺** were also investigated. As shown in Table 1, the energy levels of both HOMO and LUMO of **CzPA-F-PD-H⁺** decrease relative to those of **CzPA-F-PD**. And the LUMO level decreases more significantly. Compared to the electrochemical HOMO–LUMO gap of **CzPA-F-PD**, the energy gap in **CzPA-F-PD-H⁺** is also decreased. The results are consistent with the theoretical calculations. The hydrogen protonation on PD unit reduces the acceptor ability of the PD unit and decreases the energy level of LUMO, resulting in a bathochromic shift of the emission spectrum.

Furthermore, for discussing dual fluorescence mechanism, we also carried on spectral measurement and analysis. As expressed in Fig. S11 (ESI*), the energy level of S_1 and T_1 of were acquired in PL spectra and phosphorescence spectra. It can be drawn that the energy level gap between S_1 and T_1 (ΔE_{ST}) of **CzPA-F-PD** and **CzPA-F-PD-H⁺** is 0.39 eV and 0.16 eV, which is deduced that reverse intersystem crossing (RISC) from T_1 to S_1 doesn't happen owing to their bigger ΔE_{ST} (above 0.1 eV). And **CzPA-F-PD** and **CzPA-F-PD-H⁺** exhibit single fluorescence lifetime in Fig. S12 (ESI*), which are 2.10 ns and 2.28 ns, respectively. It is identified that dual emission of **CzPA-F-PD** is typical fluorescence. In Fig. S13 (ESI*). It can also be seen that UV-vis absorption spectrum of **CzPA-F-PD-H⁺** and PL spectrum of **CzPA-F-PD** overlap in the range of 400 nm ~ 500 nm. It means that **CzPA-F-PD-H⁺** can realize red-light emission by Förster resonance energy transfer (FRET) from **CzPA-F-PD**.

Hence, based on the above mentioned results, dual fluorescence emission process can be described as shown in Fig. 10: firstly, **CzPA-F-PD** and **CzPA-F-PD-H⁺** are excited by $h\nu_{a1}$ (i.e. $\lambda_{\text{abs}}=384$ nm) and $h\nu_{a2}$ (i.e. $\lambda_{\text{abs}}=445$ nm), respectively; then, **CzPA-F-PD** and **CzPA-F-PD-H⁺**

**Fig. 10** Diagrams of the calculated energy levels of **CzPA-F-PD** and **CzPA-F-PD-H⁺** and the simplified model for exciton relaxation processes.

realize blue-emission (i.e. $\lambda_{\text{PL}} = 470$ nm) and red-emission (i.e. $\lambda_{\text{PL}} = 620$ nm) by radiative transition of $S_1 \rightarrow S_0$, respectively; meanwhile, partial of excited energy of excited **CzPA-F-PD** molecules transfer to ground **CzPA-F-PD-H⁺** molecules by FRET, which also induces in red-emission of **CzPA-F-PD-H⁺**; eventually, dual fluorescence emission is realized.

Application of **CzPA-F-PD** as ODFMs

Fluorescence probe of pH value

Based on above discussion, it can be drawn that TFA can induce in dual fluorescence emission of **CzPA-F-PD**. Therefore, it is speculated that **CzPA-F-PD** can be utilized as fluorescence probe for pH sensing. For identifying this, pH titration experiments were performed by dropping disodium hydrogen phosphate-citric acid buffer solutions into **CzPA-F-PD** dimethyl sulfoxide (DMSO) solution (10^{-4} mol/L), and PL spectrum was recorded. As illustrated in Fig. 11a, the PL spectrum of **CzPA-F-PD** solution varies remarkably with increasing titration amount of disodium hydrogen phosphate-citric acid buffer solutions (i.e. lowering pH value). When pH values lower from 8.0 to 2.2, it is clearly observed that blue-emission peak located at 470 nm is weakened and red-emission peak located at 600 nm is enhanced, which is nearly identical with those in PL spectrum of **CzPA-F-PD** solution with increasing dropping amount of TFA. Furthermore, it can be seen in Fig. 11b that a good linear relationship between PL intensity ratio ($I_{\text{red}}/I_{\text{blue}}$) i.e. red-emission peak to blue-emission peak and pH value in the range of 2.2~8.0 is observed, which is $y=2.818-0.379x$ and $R=0.914$. Hence, it can be deduced that **CzPA-F-PD** exhibits better performance of fluorescence probe for pH sensing

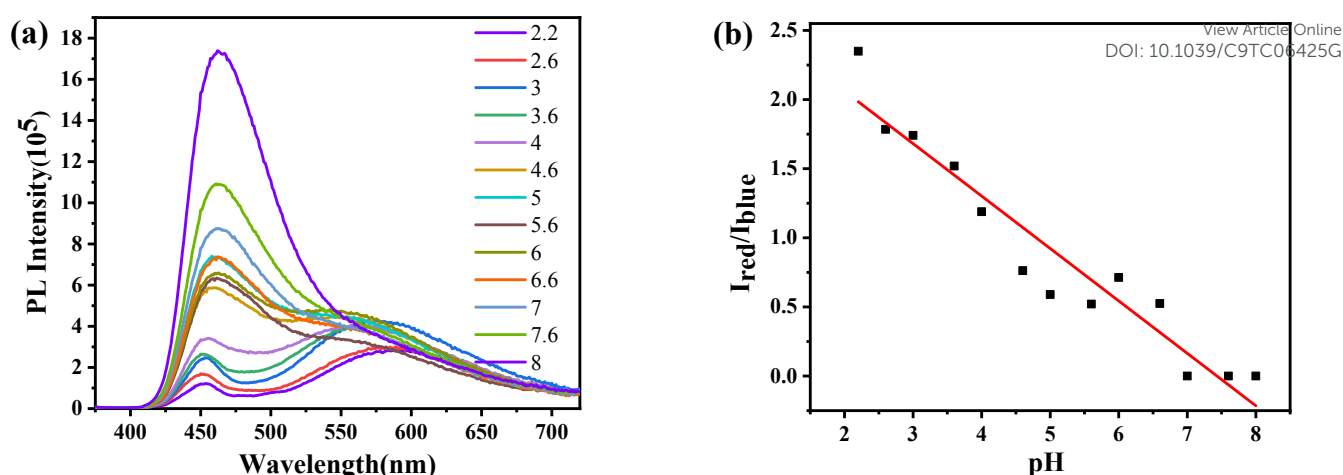


Fig. 11 (a) PL spectrum of **CzPA-F-PD** in DMSO solution (10^{-4} mol/L) with different pH values; (b) linear relationship between PL intensity ratio ($I_{\text{red}}/I_{\text{blue}}$) of red-emission peak at 600 nm to blue-emission peak at 470 nm and pH values ranging from 2.2 to 8.0.

which shows huge application in disease diagnosis and environmental protection monitoring.

Single emission layer in WOLED

Owing to dual fluorescence properties, **CzPA-F-PD** shows promising application in WOLED.^{5,38} As a proof of concept, three OLEDs were fabricated, in which TmPyPB, DPEPO, Liq and Al served as electron transporting layer, hole blocking layer, electron-injection layer and cathode. The device configurations were ITO/PEDOT: PSS/Emission Layer (50 nm)/DPEPO (10 nm)/TmPyPB (50 nm)/Liq (1 nm)/Al (100 nm). Among them, the emission layer was **CzPA-F-PD**: TFA (50/1, v: v) for Device A, **CzPA-F-PD**: TFA (5000/1, v: v) for Device B, and **CzPA-F-PD** for Device C, respectively. As shown in Fig. 12a, the EL spectra of all OLEDs exhibit a blue emission peak at around 470 nm corresponding the radiative decay from **CzPA-F-PD**. With raising content of TFA in the emission layer, the additional EL peak at the long wavelength side appears and enhances, which originates from the emission of **CzPA-F-PD-H⁺**. When the volume ratio of **CzPA-F-PD** to TFA rises to 50/1, the EL spectrum of Device A shows double emission peaks at 470 nm and 592 nm, which realizes white-light emission with CIE coordinates of (0.36, 0.37). And the Device A also exhibits excellent EL performances, e.g., the maximum luminance (L_{max}), the maximum current efficiency (CE), the maximum power efficiency (PE) and the EQE reach 1351 cd/m², 6.97cd/A, 3.65 lm/W, and 4.07%, respectively.

In addition, the maximum EQE of Device A is nearly close to 5%, inspires us to further investigate of single exciton utilization efficiency (η_s) based on the following eqn (1)

$$EQE = \gamma \times \eta_{PL} \times \eta_s \times \eta_{out} \quad (1)$$

where η_{out} is light out-coupling efficiency (≈ 0.20), γ is the ideal recombination efficiency of excitons ($\approx 100\%$), and η_{PL} is the PL efficiency of **CzPA-F-PD**: TFA (50/1, v: v) film (≈ 0.30). So, η_s of Device A is calculated to be 67.8%, which are much higher than the upper limit of η_s (25%) for traditional fluorescence. Hence, it is identified that **CzPA-F-PD** combining with the proper content of TFA can be served as single emission layer in WOLED.

Conclusions

In conclusion, **CzPA-F-PD** was synthesized with twisted A- π -D- π -A configuration. Notably, **CzPA-F-PD** shows remarkable dual fluorescence properties upon the treatment with TFA, which can also recover upon the treatment with TEA. Furthermore, it is identified that enlargement of lone pair electrons surrounding nitrogen atoms in pyridine ring by hydrogen protonation can improve electron acceptor ability of PD unit and induce in bathochromic-shift of emission spectrum eventually. In addition, it is also testified that FRET from excited molecule of **CzPA-F-PD** to ground molecule of **CzPA-F-PD-H⁺** also take place during dual fluorescence process. Based on that, a fluorescence probe for pH sensing was constructed with a linear responsivity. Furthermore, by controlling content of TFA, the **CzPA-F-PD** was employed as a single white emission layer via spin-coating for OLED applications. The experimental results prove that unique compound with the versatile functions is promising for sensing and optoelectronic applications.

Table 2 EL performance of Devices A, B, C

Device	Emitter	λ_{max} (nm)	CIE (x, y)	L_{max} (cd/m ²)	CE_{max} (cd/A)	PE_{max} (lm/W)	EQE_{max} (%)
A	CzPA-F-PD : TFA (50/1, v:v)	470,592	(0.36, 0.37)	1351	6.97	3.65	4.07
B	CzPA-F-PD : TFA (5000/1, v:v)	462,600	(0.25, 0.26)	1159	7.11	3.92	4.67

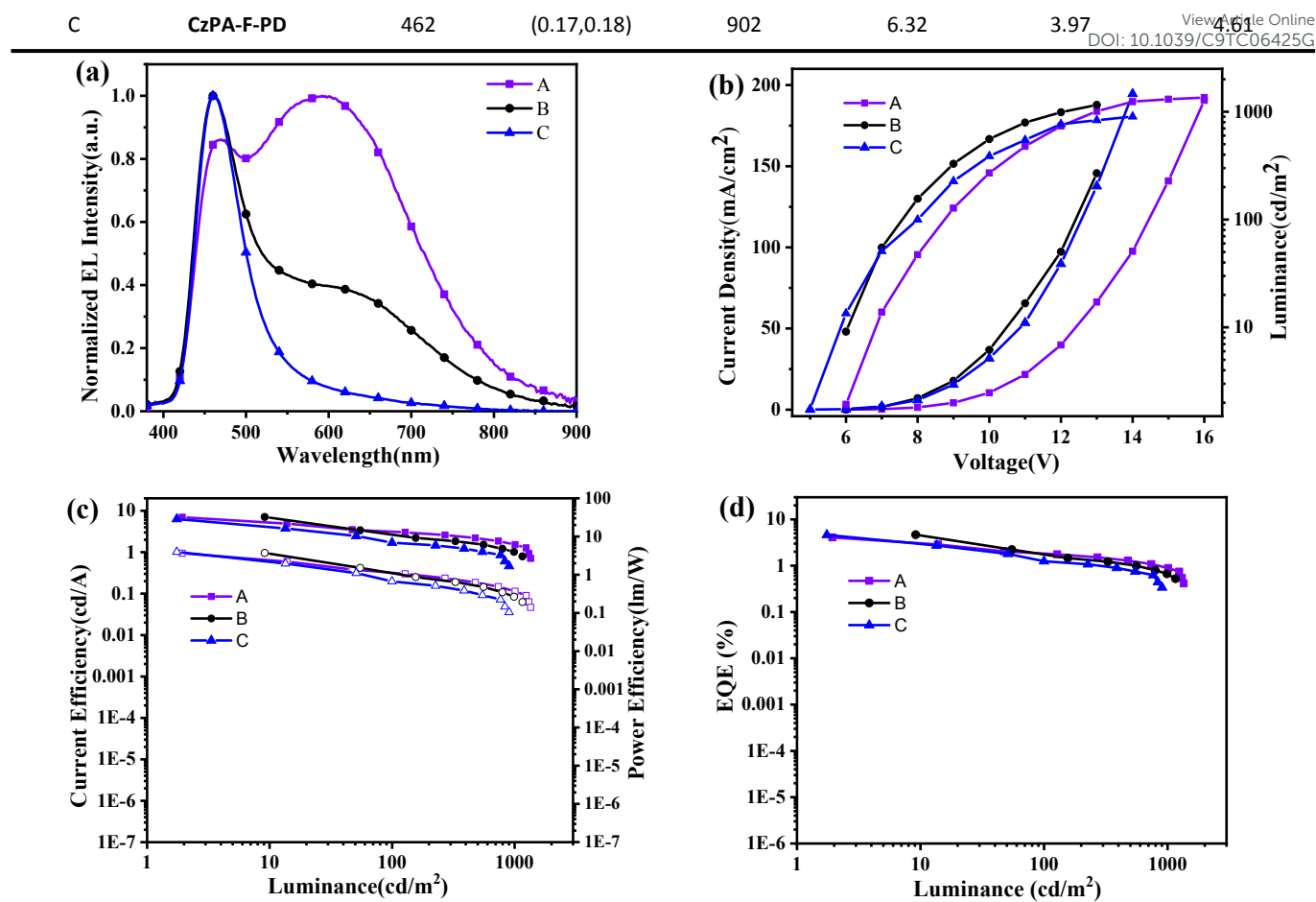


Fig. 12 (a) EL spectra; (b) J - V - L curve; (c) CE - L - PE curve and (d) EQE - L curve for Devices A, B, C.

Conflicts of interest

There are no conflicts to declare.

Acknowledgements

This work was financial supported by the National Natural Scientific Foundation of China (61775155, 61605138, 61705158), Shanxi Provincial Key Research and Development Program (201903D121100), Shanxi Provincial Key Innovative Research Team in Science and Technology (201601D021043).

References

- 1 I. Bhattacharjee, N. Acharya, H. Bhatia and D. Ray, *J. Phys. Chem. Lett.*, 2018, **9**, 2733-2738.
- 2 S. Mukherjee and P. Thilagar, *Dyes Pigm.*, 2014, **110**, 2-27.
- 3 K. C. Tang, M. J. Chang, T. Y. Lin, H. A. Pan, T. C. Fang, K. Y. Chen, W. Y. Hung, Y. H. Hsu and P. T. Chou, *J. Am. Chem. Soc.*, 2011, **133**, 17738-17745.
- 4 L. Z. Bijin Li, Hu Cheng, Quan Huang, Jingbo Lan, Liang Zhou and Jingsong You, *Chem. Sci.*, 2018, **9**, 1213-1220.
- 5 K. Wang, S. Huang, Y. Zhang, S. Zhao, H. Zhang and Y. Wang, *Chem. Sci.*, 2013, **4**, 3288-3293.
- 6 K. Wang, Y.-Z. Shi, C.-J. Zheng, W. Liu, K. Liang, X. Li, M. Zhang, H. Lin, S.-L. Tao, C.-S. Lee, X.-M. Ou and X.-H. Zhang, *ACS Appl. Mater. Interfaces*, 2018, **10**, 31515-31525.
- 7 K. P. Carter, A. M. Young and A. E. Palmer, *Chem. Rev.*, 2014, **114**, 4564-4601.
- 8 G. Zhang, G. M. Palmer, M. W. Dewhurst and C. L. Fraser, *Nat. Mater.*, 2009, **8**, 747-751.
- 9 X. Zheng, R. Fan, K. Xing, A. Wang, X. Du, P. Wang and Y. Yang, *J. Mater. Chem. C*, 2018, **6**, 6229-6239.
- 10 S. K. Dwivedi, R. C. Gupta, P. Srivastava, P. Singh, B. Koch, B. Maiti and A. Misra, *Anal. Chem.*, 2018, **90**, 10974-10981.
- 11 M. You, M. Lin, S. Wang, X. Wang, G. Zhang, Y. Hong, Y. Dong, G. Jin and F. Xu, *Nanoscale*, 2016, **8**, 10096-10104.
- 12 P. N. Anatolio Pigliucci, Abdul Rehman, Laura Gagliardi, Christopher J. Cramer, and Eric Vauthey, *J. Phys. Chem. A*, 2006, **110**, 9988-9994.
- 13 D. Li, J. Wang and X. Ma, *Adv. Opt. Mater.*, 2018, **6**, 1800273.
- 14 R. Sung and K. Sung, *J. Lumin.*, 2018, **202**, 163-167.
- 15 S. Achelle, J. Rodríguez-López, C. Katan and F. Robin-le Guen, *J. Phys. Chem. C*, 2016, **120**, 26986-26995.
- 16 F. Kournoutas, K. Seintis, N. Karakostas, J. Tydlit, S. Achelle, G. Pistolis, F. Bures and M. Fakis, *J. Phys. Chem. A*, 2019, **123**, 417-428.
- 17 M. Li, Y. Yuan and Y. Chen, *ACS Appl. Mater. Interfaces*, 2018, **10**, 1237-1243.18
- 18 S. H. Kim, S. Park, J. E. Kwon and S. Y. Park, *Adv. Funct. Mater.*, 2011, **21**, 644-651.

- 19 K. Wu, T. Zhang, Z. Wang, L. Wang, L. Zhan, S. Gong, C. Zhong, Z. H. Lu, S. Zhang and C. Yang, *J. Am. Chem. Soc.*, 2018, **140**, 8877-8886.
- 20 Z. Zhang, Y.-A. Chen, W.-Y. Hung, W.-F. Tang, Y.-H. Hsu, C.-L. Chen, F.-Y. Meng and P.-T. Chou, *Chem. Mater.*, 2016, **28**, 8815-8824.2121
- 21 K. Wang, C. J. Zheng, W. Liu, K. Liang, Y. Z. Shi, S. L. Tao, C. S. Lee, X. M. Ou and X. H. Zhang, *Adv. Mater.*, 2017, **29**, 1701476.
- 22 D.-G. Chen, T.-C. Lin, Y.-A. Chen, Y.-H. Chen, T.-C. Lin, Y.-T. Chen and P.-T. Chou, *J. Phys. Chem. C*, 2018, **122**, 12215-12221.
- 23 M. Hou, H. Wang, Y. Miao, H. Xu, Z. Guo, Z. Chen, X. Liao, L. Li, J. Li and K. Guo, *ACS Appl. Energy Mater.*, 2018, **1**, 3243-3254.
- 24 W. Li, D. Liu, F. Shen, D. Ma, Z. Wang, T. Feng, Y. Xu, B. Yang and Y. Ma, *Adv. Funct. Mater.*, 2012, **22**, 2797-2803.
- 25 W. Li, Y. Pan, L. Yao, H. Liu, S. Zhang, C. Wang, F. Shen, P. Lu, B. Yang and Y. Ma, *Adv. Opt. Mater.*, 2014, **2**, 892-901.
- 26 S. Zhang, W. Li, L. Yao, Y. Pan, F. Shen, R. Xiao, B. Yang and Y. Ma, *Chem. Commun.*, 2013, **49**, 11302-11304.
- 27 M. Cheng, J. Zhang, X. Ren, S. Guo, T. Xiao, X. Y. Hu, J. Jiang and L. Wang, *Chem. Commun.*, 2017, **53**, 11838-11841.
- 28 A. Ekbote, S. M. Mobin and R. Misra, *J. Mater. Chem. C*, 2018, **6**, 10888-10901.
- 29 L. Huang, Y. Qiu, C. Wu, Z. Ma, Z. Shen and X. Jia, *J. Mater. Chem. C*, 2018, **6**, 10250-10255.
- 30 H. V. Huynh, X. He and T. Baumgartner, *Chem. Commun.*, 2013, **49**, 4899-4901.
- 31 J. Sun, P. Xue, J. Sun, P. Gong, P. Wang and R. Lu, *J. Mater. Chem. C*, 2015, **3**, 8888-8894. View Article Online
DOI: 10.1039/C9TC06425G
- 32 Y. Duan, H. Ma, H. Tian, J. Liu, X. Deng, Q. Peng and Y. Q. Dong, *Chem. – Asian J.*, 2019, **14**, 864-870.
- 33 C. Ma, B. Xu, G. Xie, J. He, X. Zhou, B. Peng, L. Jiang, B. Xu, W. Tian, Z. Chi, S. Liu, Y. Zhang and J. Xu, *Chem. Commun.*, 2014, **50**, 7374-7377.
- 34 T. Liu, L. Zhu, C. Zhong, G. Xie, S. Gong, J. Fang, D. Ma and C. Yang, *Adv. Funct. Mater.*, 2017, **27**, 1606384.
- 35 X. Tang, Q. Bai, Q. Peng, Y. Gao, J. Li, Y. Liu, L. Yao, P. Lu, B. Yang and Y. Ma, *Chem. Mater.*, 2015, **27**, 7050-7057.
- 36 R. Kumar Konidena, K. R. Justin Thomas, D. Kumar Dubey, S. Sahoo and J. H. Jou, *Chem. Commun.*, 2017, **53**, 11802-11805.
- 37 D. Li, W. Hu, J. Wang, Q. Zhang, X. M. Cao, X. Ma and H. Tian, *Chem. Sci.*, 2018, **9**, 5709-5715.
- 38 D. Liu, Z. Zhang, H. Zhang and Y. Wang, *Chem. Commun.*, 2013, **49**, 10001-10003.
- 39 Q. Y. Yang and J. M. Lehn, *Angew. Chem., Int. Ed.*, 2014, **53**, 4572-4577.
- 40 L. Wang, M.-F. Lin, W.-K. Wong, K.-W. Cheah, H.-L. Tam, Z.-Q. Gao and C. H. Chen, *Appl. Phys. Lett.*, 2007, **91**.
- 41 C. Liu, Q. Fu, Y. Zou, C. Yang, D. Ma and J. Qin, *Chem. Mater.*, 2014, **26**, 3074-3083.
- 42 X. Qiu, S. Ying, C. Wang, M. Hanif, Y. Xu, Y. Li, R. Zhao, D. Hu, D. Ma and Y. Ma, *J. Mater. Chem. C*, 2019, **7**, 592-600.

Dual emission of a blue fluorescence material and its application in WOLED and fluorescence probe are investigated.

View Article Online
DOI: 10.1039/C9TC06425G

